Received September 30, 2019, accepted October 22, 2019, date of publication October 24, 2019, date of current version November 6, 2019.

Digital Object Identifier 10.1109/ACCESS.2019.2949386

Analysis of the Effect of UV-LIGA Fabrication Error on the Microspring Elastic Coefficient

YU QIN[1], LIANGYU CHEN[1], YONGPING HAO[2], SHUANGJIE LIU[2], AND XIANLONG HU[3]

[1]School of Mechanical Engineering and Automation, Northeastern University, Shenyang 110819, China
[2]School of Mechanical Engineering, Shenyang Ligong University, Shenyang 110159, China
[3]Huaihai Industries Group Company Ltd., Changzhi 046000, China

Corresponding author: Yu Qin (qinyu490@163.com)

This work was supported in part by the Natural Science Fund Guidance Program of Liaoning Province of China under Grant 20170540791.

ABSTRACT The manufacturing process of planar microsprings by the UV-LIGA process was introduced; the mechanism of fabrication error was analyzed from three process stages of exposure, SU-8 swelling, and corrosion; and the corresponding improvement measures were proposed. The line width of two groups of microsprings after the exposure, SU-8 swelling, and debonding was measured, and the elastic coefficients in three coordinate directions were accurately measured. The results show that the factors that affect the line width error are stable. The effects of the exposure diffraction, swelling of SU-8 glue, and debonding corrosion process on the line width size follow the order: corrosion error > swelling error > exposure error. When the line width is small, the aspect ratio of the microspring is large, and the direction of machining error is generally negative. The relative error of the elastic coefficient of microsprings in three coordinate directions is larger. The influence rule of the line width error on the elastic coefficient follows the order: $k_{\text{error}}y > k_{\text{error}}x > k_{\text{error}}z$.

INDEX TERMS UV-LIGA process, microsprings, fabrication error, elastic coefficient, error compensation.

I. INTRODUCTION

With the rapid development of MEMS technology, more attention has been paid to the application of MEMS devices in micromechanical structures [1], [2]. Planar microspring is a typical MEMS device, whose elasticity in three coordinate directions is essential and is widely used in carbon nanotubes, micro-inertial switches, micro-accelerometers, microgyroscopes, and other materials and devices [3]–[9]. The S-shaped microspring is a commonly used plane microspring, and the elastic coefficient is an important parameter that affects its mechanical properties [10] The elastic coefficient of microsprings is determined by the shape, structure, size, and material, and the structural parameter analysis of the spring indicates that the linewidth is the main factor that affects its elastic coefficient [11], [12]. The fabrication error during microsprings preparation, especially the line width error, affects the elastic coefficient of the microsprings. Specifically, when the error is large, the actual value may be far from the design value, which leads to a greater change in the mechanical properties of microsprings or even failure of its function. Because mechanical properties are limited by factors such as scale effects and microprocessing techniques on the microscale [13], [14], it is difficult to accurately measure the elasticity coefficient of S-shaped microsprings. Currently, most researchers use many weights to calibrate by grade [15], and a Tytron 250 microtension testing machine [16], [17] is used to obtain the microspring elastic coefficient, which has the disadvantages of not accurately centering the sample, not directly measuring the elastic coefficient, long test time, low measuring efficiency, and measuring only the longitudinal elastic coefficient. Therefore, previous literature on the effect of microsprings fabrication error on the elastic coefficient is mainly concentrated on theoretical calculations. Li et al. [18] designed and manufactured an S-shaped nickel microspring by the LIGA process, deduced the calculation formula of its elastic coefficient in three coordinate directions, analyzed the effect of the fabrication error of each structural parameter of the microspring on its mechanical properties, and pointed out that the linewidth error considerably affects its mechanical properties. Shao et al. [19] performed an accurate measurement of the linewidths of two groups of different microsprings processed by the LIGA process, calculated the longitudinal elastic coefficients by theoretical formulas, and

The associate editor coordinating the review of this manuscript and approving it for publication was Sanket Goel.

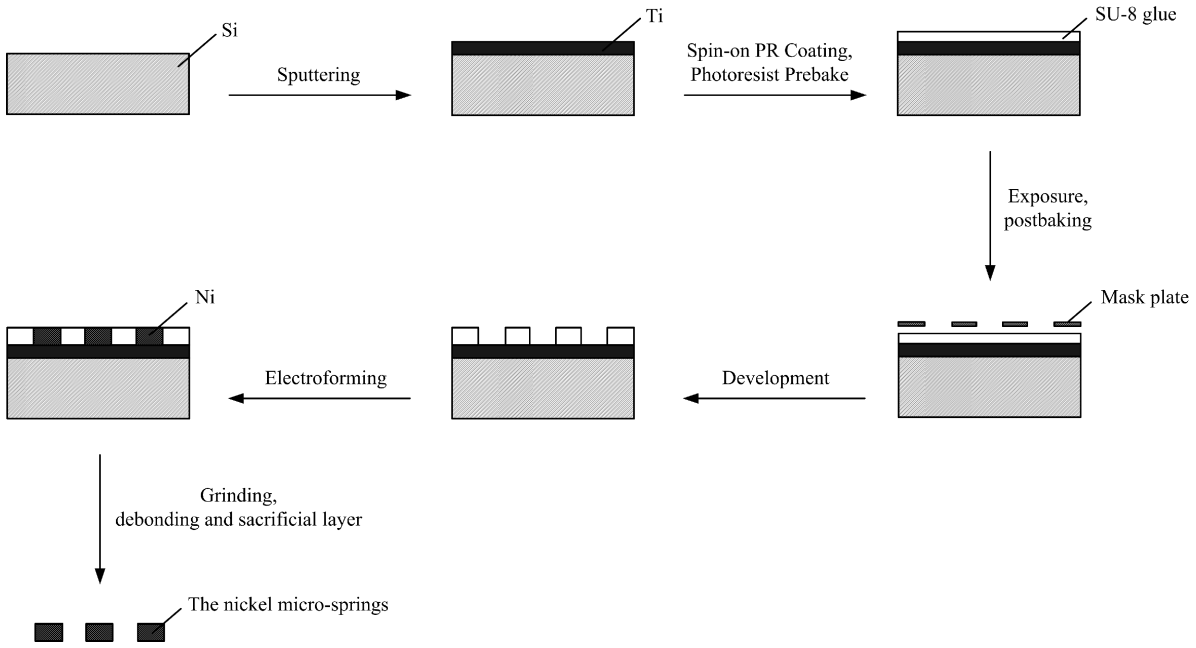

FIGURE 1. Flow chart of the microsprings preparation process.

analyzed the effect of linewidth error on longitudinal elastic coefficients. Deng et al. [20] measured the microspring size and response threshold of a MEMS inertial universal switch with flexible electrodes, analyzed the effect of processing error on the switch response threshold, and concluded that the microspring line width error was the main factor that affected the switch response threshold.

In this paper, the linewidth of two groups of microsprings made by the UV-LIGA process was measured. The influence of diffraction effect, swelling effect of the SU-8 glue and debonding corrosion process on the linewidth size was studied, and the influence of linewidth error on the elastic coefficient of microsprings in three coordinate directions was analyzed using the self-designed testing system of the elastic coefficient of microsprings to optimize the design and improve the process, to ensure the consistency of the actual mechanical properties of microsprings with the design requirements to the greatest extent, and to facilitate the mass standardized production of microsprings.

II. PREPARATION OF PLANAR MICROSPRINGS

Planar microsprings were prepared by the UV-LIGA process, which is a quasi-LIGA process that is based on the SU-8 glue. It uses ultraviolet lithography instead of synchrotron radiation X-ray lithography, which greatly reduces the processing cost and shortens the processing cycle [21]. Fig. 1 shows the process flow diagram of the metal nickel microsprings preparation, and its detailed process flow is as follows.

(1) Substrate pretreatment: The substrate is a silicon wafer, and the sacrificial layer is metal titanium. Titanium is sputtered on the silicon wafer and oxidized to increase the adhesion of the SU-8 glue to the silicon wafer. The substrate is grinded and polished by a grinding and polishing machine. Then, the substrate is immersed in acetone and ethanol solutions and cleaned by an ultrasonic cleaning machine. Finally, the substrate is washed with deionized water and dried in an oven.

(2) Spin-on PR Coating: The SU-8 glue (SU-8 2025), which is used during the preparation of microsprings, is produced by the MicroChem Company in the United States, and it was deposited at the center of the substrate. Because the viscosity of the SU-8 glue is high, a glue spinning machine made by the Karl Suss company in Germany was used, and the glue spinning method of gradual acceleration was adopted. The initial speed of glue spinning was 300 r/min, and it was increased to 650 r/min in 5 s after maintaining this speed for 10 s. Then, the speed was decreased naturally in 15 s to allow the SU-8 glue to evenly coat the substrate. Then, the SU-8 glue and the substrate were allowed to rest for approximately 30 s to weaken the "edge bead effect" [22], which appears during the spin-on PR coating process.

(3)Photoresist Prebake: The substrate with the SU-8 glue was put into a program-controlled oven for photoresist prebake. To achieve the desired effect, a stepwise heating approach was adopted. First, the temperature was adjusted to 65°C for prebaking for 30 min. Then, the temperature was increased to 85°C to dry the glue for 60 min to control the volatilization rate of the solution and improve the binding force of the SU-8 glue and the substrate. Finally, the SU-8 glue and the substrate were removed and allowed to cool to room temperature.

(4) Exposure: The SU-8 film, which was formed after the photoresist prebake, was exposed through a mask plate using a SUSS UV lithography machine at an exposure dose of 450 mJ/cm^2 and an exposure time of 45 s.

(5) Postbaking: The SU-8 glue needs to be postbaked after the exposure. Specifically, the SU-8 glue film is placed on a hot plate for baking; the temperature is set to 85°C for 2 min 30 s; then, the hot plate is closed to cool the SU-8 glue.

(6) Development: The SU-8 glue, which was cooled to room temperature, was immersed into a special developing solution and slightly stirred for 2∼4 min. The residual developer solution and the glue film residue on the SU-8 glue were washed with an ethanol solution, rinsed with an ethanol solution, rinsed again with deionized water, and finally dried with a nitrogen gas gun.

(7) Electroforming: The anode of a precision electroforming machine is made of a high purity nickel plate, and the electroforming solution is made of a nickel sulfamate solution with a specific composition. The process conditions were as follows: the voltage was 5 V, the temperature was 50°C, and the electroforming time was 4 h.

(8) Grinding: The metal surface after electroforming is not uniform. Sand paper with a large particle size was used to grind the casting layer, remove the surface defects of the casting layer, and ensure the uniform height of the casting layer. The casting coating was ground using a coarse-grained sandpaper to remove the surface defects of the casting coating while ensuring the uniform height of the casting coating. Then, the casting coating was wiped clean with an alcohol cotton ball, and after baking rinsed with deionized water.

(9) Debonding and sacrificial layer: The finished structure was put into a boiling inorganic acid, and the SU-8 glue and titanium sacrificial layer were dissolved. The structure was taken out and washed with deionized water to obtain the desired metal microsprings.

III. ERROR MECHANISM AND IMPROVEMENT MEASURES

Due to the limitations of the UV-LIGA process, the errors in microsprings are inevitable [23], which are primarily derived from three stages of the UV-LIGA process: ''diffraction effect'' [24] and ''edge bead effect'' [22] during the exposure, swelling of the SU-8 glue during the development and electroforming [25], and the debonding corrosion process.

A. EXPOSURE ERROR

In addition, due to contact exposure, there is an ''edge bead effect'' [22] during the spin-on PR coating process, and the thickness of the glue film in the middle area is smaller than that at the edge, which results in a certain gap between the mask plate and the SU-8 glue surface in the middle area, and the gap gradually increases along the thickness direction of the SU-8 glue. This phenomenon causes contact exposure to become a close exposure with a certain gap, which results in a certain dimensional error. The inclination angle of the sidewall of the SU-8 glue during the exposure process is the third factor that causes the exposure error. There is no linear relationship between the variation of the SU-8 glue linewidth and exposure time [26], and the variation of linewidth is different at the top and bottom due to different exposures. Because the amount of light at the bottom is less than that at the top, the bottom SU-8 glue polymerizes less than that at the top, which results in a bottom line width that is smaller than the top line width [27]. Fig. 2 shows the difference between the actual imaging size of the SU-8 glue and the mask pattern size after the exposure. In the figure, B_0 is the characteristic width of the mask plate graphic, a is the top linewidth offset of the SU-8 glue, b is the bottom linewidth offset, G is the gap between the mask plate and the surface of the SU-8 glue, H is the thickness of the SU-8 glue, and α is the sidewall inclination.

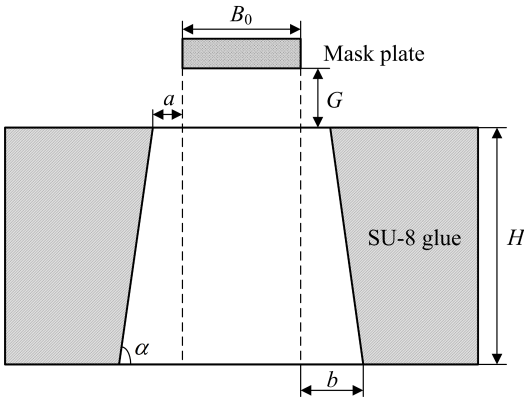

FIGURE 2. Schematic diagram of the actual imaging size and mask pattern size after the exposure.

1) IMPROVEMENT MEASURES

(1) It is essential to select a suitable organic material (e.g., glycerin) to fill between the mask plate and the SU-8 glue to reduce the gap between the mask and the SU-8 glue [28];

(2) The sidewall inclination angle of the SU-8 glue is increased using multiple oblique exposures or back exposures [29];

(3) A hard contact exposure mode is adopted.

B. SU-8 SWELLING ERROR

During development and electroforming, the solution molecules penetrated into the SU-8 glue to change the structure size, which is called swelling of the SU-8 glue [25]. The swelling error is mainly caused by the inclination angle of the sidewall. The inclination angle occurs because the exposure amount at the top and bottom of the SU-8 glue is different during the exposure process, and the polymer structure produced by the bottom polymerization is looser than that at the top, which is easier to swell during the subsequent development and electroforming process. However, because the bottom of the SU-8 film is constrained by the sacrificial layer, the offset at the junction of sacrificial layer is 0 during swelling, which leads to the linewidth at the bottom of the SU-8 film to be smaller than that at the top, and the casting layer exhibits a trapezoidal structure with narrow upper and wide lower boundaries. Fig. 3 is a schematic diagram of the swelling of the SU-8 glue, in which B_0 is the characteristic

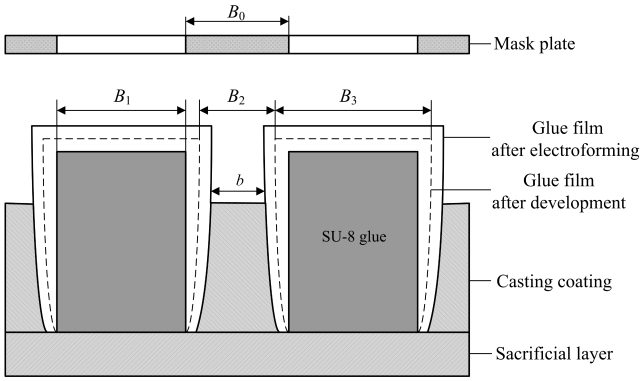

FIGURE 3. Schematic diagram of SU-8 swelling.

width of the mask plate pattern, B_1 is the design line width of the SU-8 film, B_2 is the actual width of the top of the adhesive film channel after development, B_3 is the actual width of the top of the adhesive film after development, and b is the actual width of the top of the casting layer after electroforming; $\delta_1 = B_3 - B_1$ is the size error of the adhesive film during development, $\delta_2 = B_2 - b$ is the dimensional error of the adhesive film during electroforming, $\delta = B_0 - b$ is the size error of microsprings after electroforming.

1) IMPROVEMENT MEASURES

(1)It is essential to reduce the electroforming temperature to reduce the thermal expansion of the SU-8 adhesive film [30];

(2)Ultrasonic treatment is introduced during the development and electroforming process, and the strong mechanical action of ultrasonic waves is used to break the chemical bonds in the molecular chain of the SU-8 glue; the free volume in the glue is reduced, and the solution is not easy to diffuse in the glue, which reduces the swelling of the glue [31];

(3)An isolation channel is arranged around the electroforming structure to prevent the influence of the swelling of the peripheral large area SU-8 glue [32].

C. CORROSION ERROR

Due to the excellent thermal and chemical stability of the SU-8 glue, the postbaked SU-8 glue forms a dense cross-linking network. This cross-linking network is highly resistant to solvents and acid-base solutions and resists expansion, which makes the removal of the SU-8 glue very difficult. [33] In this paper, the inorganic acid corrosion method is used to remove the SU-8 glue. Although metal nickel possesses strong corrosion resistance to strong acids, inorganic acids still cause a certain corrosion to the structure of microsprings, which results in dimensional error.

1) IMPROVEMENT MEASURES

It is essential to introduce the method of dimensional error compensation and determine the compensation amount according to the experimental and empirical values during processing. In addition, the mask line width of microsprings needs to be appropriately added.

IV. ERROR MEASUREMENT AND ANALYSIS

A. SAMPLE PREPARATION

Microspring consists of n units with identical structures, each of which is shown in Fig. 4, with B being the line width of the spring. Fig. 5 shows an intelligent digital automatic stereoscopic microscope. It can be used to measure the size of each microspring unit. Two groups of nickel microsprings prepared by the UV-LIGA process were analyzed, marked # 1 and # 2. The design values of line widths of the two groups are 10 μm and 40 μm respectively. The design value of the aspect ratio is 8, and the number of spring segments is 12. The EMS photographs are shown in Fig. 6.

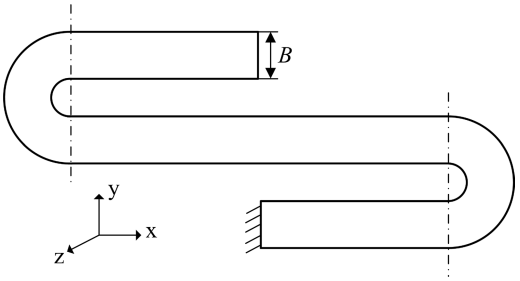

FIGURE 4. Unit model of microsprings.

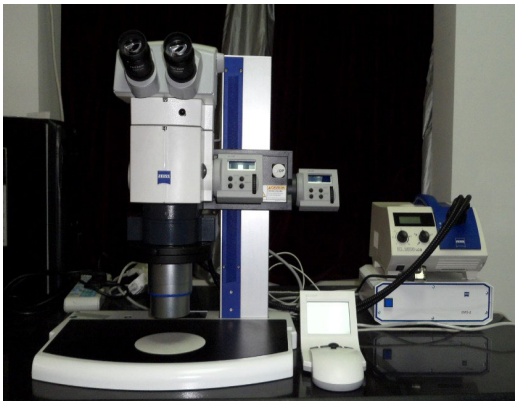

FIGURE 5. Intelligent digital automatic stereoscopic microscope.

B. MEASUREMENT RESULTS

Each group of springs requires 50 measuring line widths and uses the average value of the measured values as the line width of the spring to be measured. Fig. 7 is the line width measurement result of the microspring preparation process. Fig. 8 is the aspect ratio of the two groups of microsprings before debonding corrosion; Table 1 is the line width error range calculated according to the measurement result. The measurement results show that the corrosion error has the greatest influence on the line width during the preparation of

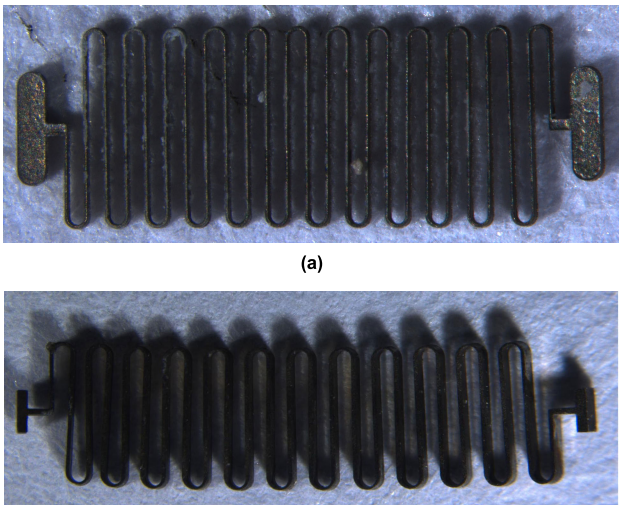

FIGURE 6. EMS photograph of microsprings. (a) #1 group; (b) #2 group.

TABLE 1. Range of the line width error.

Group	Exposure/μm	SU-8 Swelling/μm	Debonding/μm
#1	-1.09～0.43	-2.38～0.49	-3.97～-0.35
#2	-1.15～0.93	-1.28～2.28	-2.74～2.1

the microspring, and the exposure error has the least influence on the line width. The aspect ratio of group # 1 before debonding is greater than that of group # 2. Negative deviation occurs during debonding corrosion, and the measured value of line width after debonding is less than the design value. Because the line width of group # 1 is smaller and the aspect ratio is larger, the time spent in the depth direction is longer than that in the line width direction when debonding, and the size of the line width part is excessively corroded, which leads to the deviation with a consistent trend.

C. ERROR ANALYSIS

Table 2 shows the main dimensions of the line width measurement. Table 2 shows that the measured values of the two groups of microsprings fall within the tolerance range, which satisfies the "3σ criterion" [34]. Fig. 9 is the histogram of the line width measurement values and the fitted normal distribution curve. It can be seen from the figure that most of the measurement values are concentrated near the average value; the data consistency is good and close to the normal distribution, which indicates that the factors that affect

TABLE 2. Main dimensions of the line width measurements.

Group	#1	#2
Average Value/μm	7.66	40.32
Standard Deviation/μm	0.78	1.32
Minimum Value/μm	6.03	37.26
Maximum Value/μm	9.65	42.1
Tolerance Range/μm	5.32~10	36.36~44.28

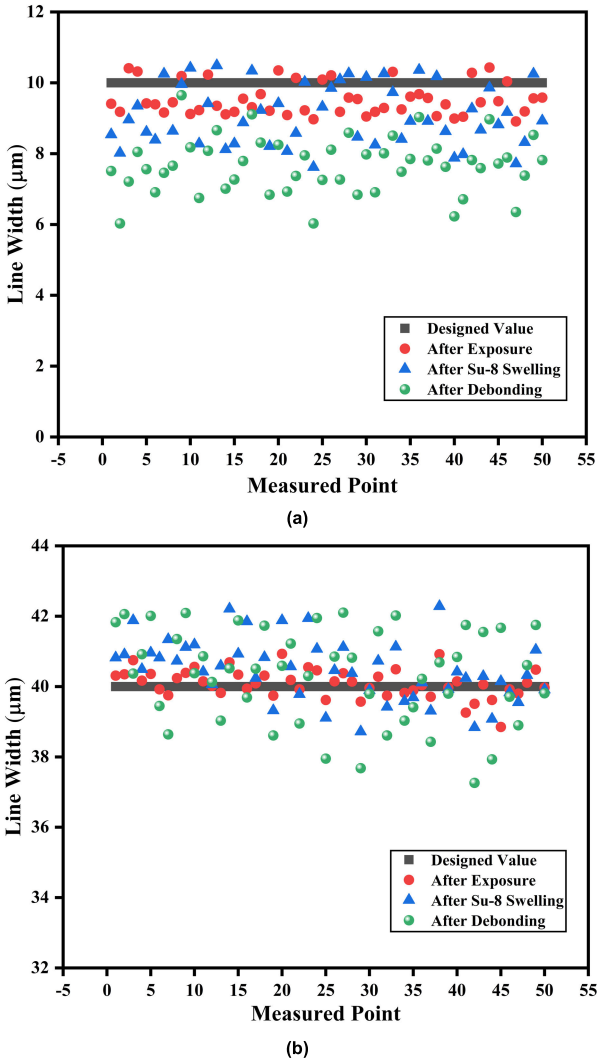

FIGURE 7. Line width measurement of microsprings. (a) #1 group; (b) #2 group.

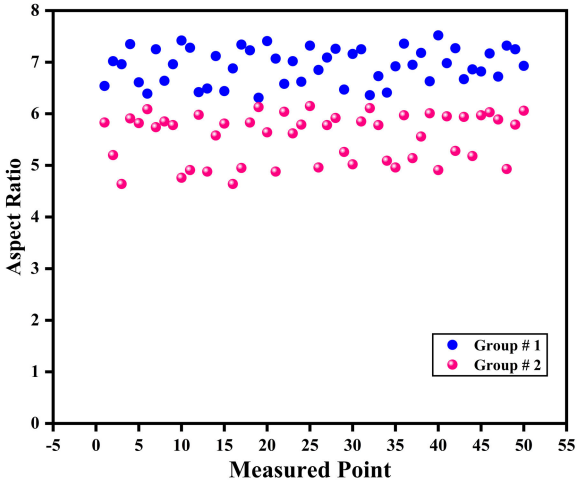

FIGURE 8. Aspect ratio before debonding.

the line width fabrication error during the process of spring preparation are stable, and the error can be reduced by error compensation.

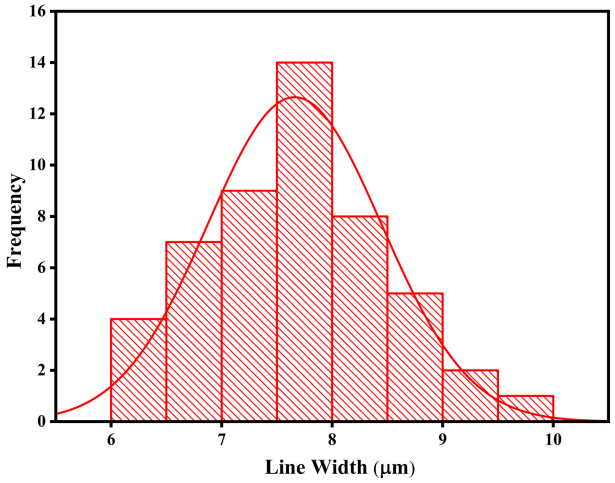

(a)

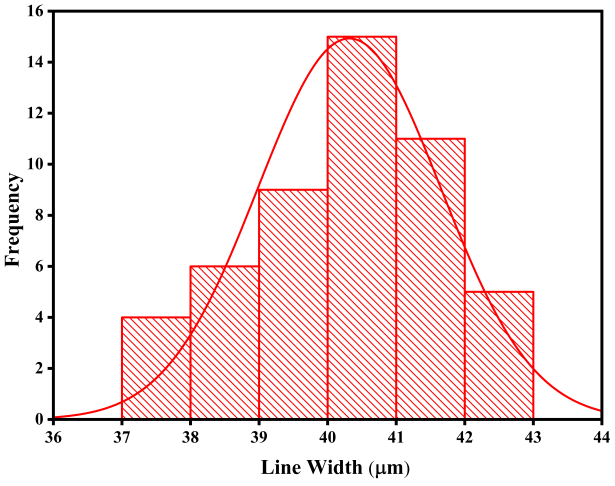

(b)

FIGURE 9. Histogram and normal fitting curve of the linewidth measurement. (a) #1 group; (b) #2 group.

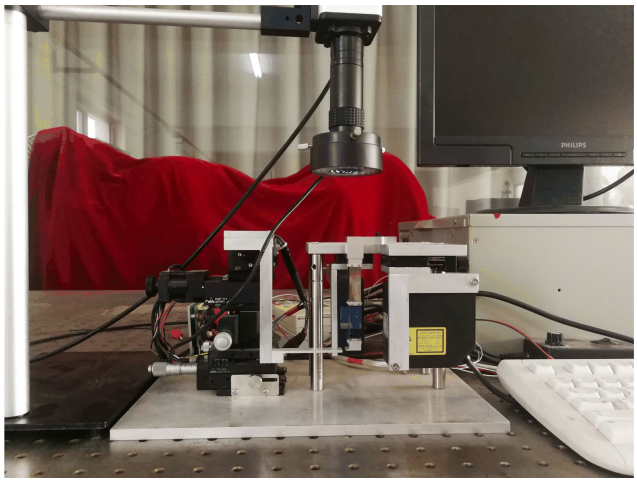

FIGURE 10. A picture of the micro-spring testing system.

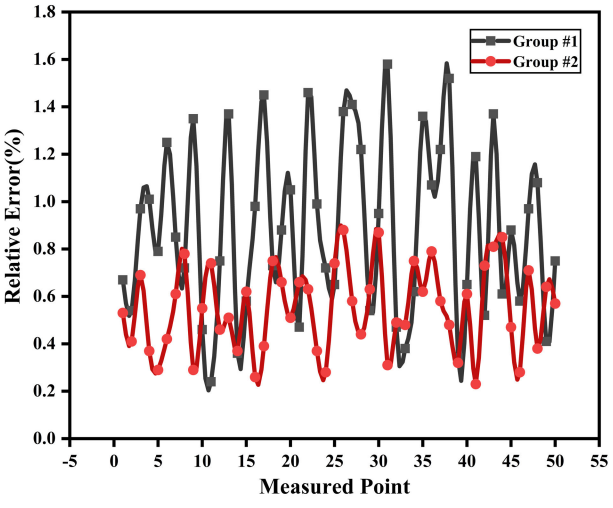

(a)

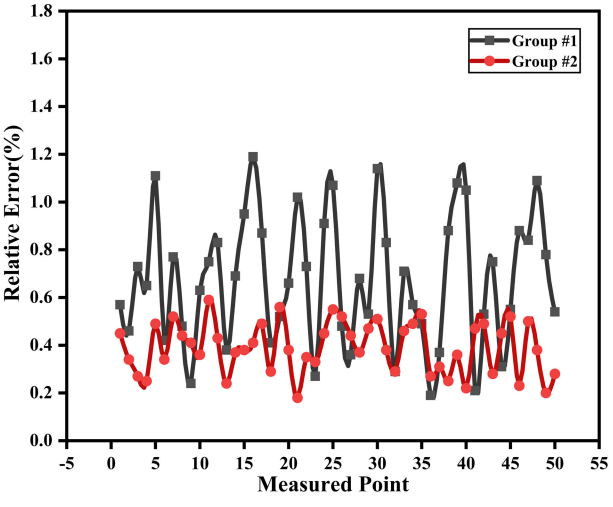

(b)

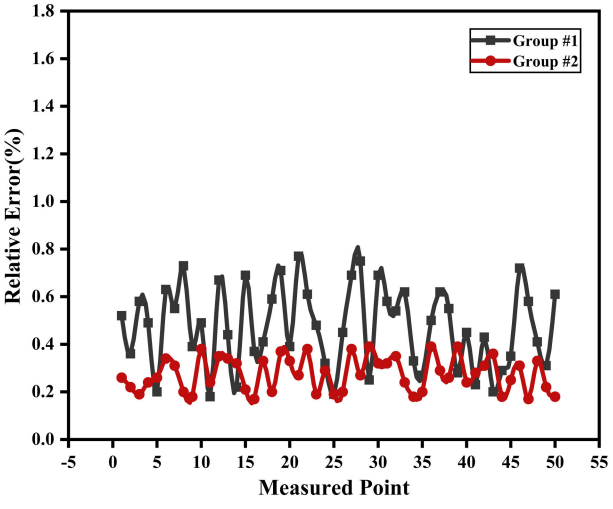

(c)

FIGURE 11. Comparison of relative errors of elastic coefficients. (a) *y* direction; (b) *x* direction; (c) *z* direction.

V. ELASTIC COEFFICIENT TEST

To solve the problem that the effect of fabrication error on the elastic coefficient is difficult to detect online, Fig. 10 shows the self-designed microspring testing system of elastic coefficients [35] that can achieve automatic leveling of microsprings and fundamentally remove uncertainties that

TABLE 3. Elastic coefficient design value.

Group	y direction(N/m)	x direction(N/m)	z direction(N/m)
#1	0.589	0.111	0.277
#2	19.898	0.428	3.518

are caused by the failure to accurately center sample pieces in the current testing system. The accurate testing of elastic coefficients in the x, y, and z directions of the microspring can be realized by automating electric microdisplacement tables via the main control computer, and the defects that are present in the existing method for obtaining the elastic coefficient of microsprings are overcome. Table 3 shows the design values of the elastic coefficients of two groups of microsprings. The elastic coefficients of the two groups in the x, y, and z directions are tested using the test system shown in Fig. 10. This paper only considers the test in the linear range of the microsprings and plots the relative error values between the test results of each group and the original design values as shown in Figs. 11 (a) $\sim$ (c). These figures show that the variation range of the x, y, and z directions of the #1 group microsprings is larger than that of the #2 group, which indicates that the relative error of the elastic coefficient of the #1 group microsprings is relatively large. In addition, it is observed that the variation amplitude of the y direction relative error curves of the two groups is larger than that of the x and z directions, which shows that the linewidth error has the greatest effect on the y direction elastic coefficient of microsprings.

VI. CONCLUSION

In this paper, the line widths of two groups of microsprings prepared by the UV-LIGA process were measured, and the elastic coefficients of three coordinate directions were accurately measured.

(1) The factors that affect the line width error during the process of microspring fabrication are stable. The effects of the exposure diffraction effect, swelling effect of the SU-8 glue, and the debonding corrosion process on the line width size follow the order: corrosion error $>$ swelling error $>$ exposure error.

(2) Under the same processing method and test conditions, a microspring with a smaller line width has a larger aspect ratio, and its processing error direction is generally negative. Thus, the positive deviation processing method can compensate for the error during the actual process.

(3) The relative error of the elastic coefficient of microsprings with a smaller line width is larger in three coordinate directions. The effect of the line width fabrication error on the elastic coefficient follows the order: $k_{\text{error}}y > k_{\text{error}}x > k_{\text{error}}z$.

REFERENCES

[1] W. J. Park, J. W. Song, C. H. Kang, J. H. Lee, M. H. Seo, S. Y. Park, J. Y. Yeo, and C. G. Park, "MEMS 3D DR/GPS integrated system for land vehicle application robust to GPS outages," *IEEE Access*, vol. 7, pp. 73336–73348, 2019.

[2] H. Pezous, C. Rossi, M. Sanchez, F. Mathieu, X. Dollat, S. Charlot, L. Salvagnac, and V. Conédéra, "Integration of a MEMS based safe arm and fire device," *Sens. Actuators A, Phys.*, vol. 159, no. 2, pp. 157–167, 2010.

[3] K. S. Rao, L. N. Thalluri, K. Guha, and K. G. Sravani, "Fabrication and characterization of capacitive RF MEMS perforated switch," *IEEE Access*, vol. 6, pp. 77519–77528, 2018.

[4] S. Kalaiselvi, L. Sujatha, and R. Sundar, "Fabrication of MEMS accelerometer for vibration sensing in gas turbine," in *Proc. IEEE SENSORS*, Oct. 2018, pp. 1–4. [Online]. Available: https://ieeexplore.ieee.org/abstract/doc ument/8589799

[5] H. Cao, Y. Liu, Y. Zhang, X. Shao, J. Gao, K. Huang, Y. Shi, J. Tang, C. Shen, and J. Liu, "Design and experiment of dual-mass MEMS gyroscope sense closed system based on bipole compensation method," *IEEE Access*, vol. 7, pp. 49111–49124, 2019.

[6] M. Ö. Yayli, "Buckling analysis of a cantilever single-walled carbon nanotube embedded in an elastic medium with an attached spring," *Micro Nano Lett.*, vol. 12, pp. 255–259, Dec. 2016.

[7] M. Ö. Yayli, "Free longitudinal vibration of a nanorod with elastic spring boundary conditions made of functionally graded material," *Micro Nano Lett.*, vol. 13, pp. 1031–1035, Apr. 2018.

[8] M. O. Yayli, "On the axial vibration of carbon nanotubes with different boundary conditions," *IET Micro Nano Lett.*, vol. 9, no. 11, pp. 807–811, 2014.

[9] M. Ö. Yayli, "Free vibration analysis of a single-walled carbon nanotube embedded in an elastic matrix under rotational restraints," *Micro Nano Lett.*, vol. 13, pp. 202–206, Sep. 2017.

[10] G. Li, L. Sui, and G. Shi, "Study on the Linearly Range of S-Shaped MEMS Planar Micro-spring," *Proc. TELKOMNIKA*, vol. 10, no. 6, pp. 1327–1332, Oct. 2012.

[11] W. Nie, J. Cheng, Z. Xi, Z. Zhou, and L. Yin, "Elastic coefficient analysis on planar S-shaped micro spring under high impact load," *Microsyst. Technol.*, vol. 23, no. 5, pp. 1367–1375, May 2017.

[12] Z. Yang, G. Ding, H. Cai, S. F. Gang, and X. Zhao, "Finite element dynamics analysis of micro-spring in MEMS inertia switch," *J. Mechan. Streng.*, vol. 30, no. 4, pp. 586–589, May 2008.

[13] T. Ando, M. Shikida, and K. Sato, "Tensile-mode fatigue testing of silicon films as structural materials for MEMS," *Sens. Actuators A, Phys.*, vol. 93, no. 1, pp. 70–75, Aug. 2001.

[14] M. Shavezipur, K. Ponnambalam, A. Khajepour, and S. M. Hashemi, "Fabrication uncertainties and yield optimization in MEMS tunable capacitors," *Sens. Actuators A, Phys.*, vol. 147, no. 2, pp. 613–622, Oct. 2008.

[15] L. Shi, J. Li, D. Chen, Z. Ni, and J. Zhu, "Fabrication and characterization of S-form MEMS planer micro-springs," *Tech. Pro.*, vol. 1, pp. 19–21, Jan. 2004.

[16] H. Li and G. Shi, "Contrastive study on the mechanical performance of MEMS microsprings fabricated by LIGA and UV-LIGA technology," *Proc. SPIE*, vol. 3, Jan. 2008, Art. no. 68360E. [Online]. Available:https://www.spiedigitallibrary.org/conference-proceedings -of-spie/68360E/Contrastive-study-on-the-mechanic-al-performance-of -MEMS-microsprings-fabricated/10.1117/12.756048.short?SSO=1

[17] H. Li and S. Gengchen, "Analysis of application patterns of Z-type MEMS microspring," *Microsyst. Technol.*, vol. 15, no. 4, pp. 527–533, Apr. 2009.

[18] H. Li, G. Shi, and G. He, "Analysis of effect of MEMS fabrication error on the microspring mechanical property," *Piezo. Acoust.*, vol. 31, no. 5, pp. 735–741, Oct. 2009.

[19] W. Shao, J. Zhang, Y. Hao, Y. Qu, W. Wang, and S. Gu, "Analysis of dimension tolerance for MEMS Ni planar micro spring," *J. Mach. Des.*, vol. 29, no. 8, pp. 80–82, Aug. 2012.

[20] P. Deng, Y. Wu, and Y. Hao, "Analysis of fabracation error on MEMS Om-nidirectional trigger," *J. Ordnance Equip. Eng.*, vol. 37, no. 10, pp. 110–113, Oct. 2016.

[21] W. Qu, C. Wenzel, A. Jahn, and D. Zeidler, "UV-LIGA: A promising and low-cost variant for microsystem technology," in *Proc. Conf. Optoelectron. Microelectron. Mater. Devices*, Dec. 1998, pp. 380–383. [Online]. Available: https://ieeexplore.ieee.org/abstract/document/791668

[22] L. Du, M. Zhao, A. Wang, S. Chen, and W. Nie, "Fabrication of novel MEMS inertial switch with six layers on a metal substrate," *Microsyst. Technol.*, vol. 21, no. 9, pp. 2025–2032, Sep. 2015.

[23] R. Liu, B. Paden, and K. Turner, "MEMS resonators that are robust to process-induced feature width variations," *J. Microelectromech. Syst.*, vol. 11, no. 5, pp. 505–511, Oct. 2002.

[24] R. Lawes, "Manufacturing tolerances for UV LIGA using SU-8 resist," *J. Micromech. Microeng.*, vol. 15, pp. 2198–2203, Oct. 2005.

[25] L. Yi, W. Xiaodong, L. Chong, L. Zhifeng, C. Denan, and Y. Dehui, "Swelling of SU-8 structure in Ni mold fabrication by UV-LIGA technique," *Microsyst. Technol.*, vol. 11, no. 12, pp. 1272–1275, Nov. 2005.
[26] Z. G. Ling, K. Lian, and L. Jian, "Improved patterning quality of SU-8 microstructures by optimizing the exposure parameters," *Proc. SPIE*, vol. 17, pp. 1019–1027, Jun. 2000. [Online]. Available: https://www.spied-igitall-ibrary.org/conference-proceedings-of-99/0000/Improved-patte-r-ning–quality-of-SU-8-microstructures-by-optimizing-the/10.1117/12.388266.short?SSO=1
[27] Y. Zhang, D. Chen, J. Zhang, Z. Ni, J. Zhu, and J. Liu, "Process optimization of optical lithography of SU-8 photoresist," *Microfabr. Technol.*, vol. 5, no. 3, pp. 36–41, Mar. 2005.
[28] Y.-J. Chuang, F.-G. Tseng, and W.-K. Lin, "Reduction of diffraction effect of UV exposure on SU-8 negative thick photoresist by air gap elimination," *Microsyst. Technol.*, vol. 8, nos. 4–5, pp. 308–313, Aug. 2002.
[29] M. Han, W. Lee, S.-K. Lee, and S. Lee, "3D microfabrication with inclined/rotated UV lithography," *Sens. Actuators A, Phys.*, vol. 111, no. 1, pp. 14–20, Mar. 2004.
[30] A. Ruzzu and B. Matthis, "Swelling of PMMA-structures in aqueous solutions and room temperature Ni-electroforming," *Microsyst. Technol.*, vol. 8, nos. 2–3, pp. 116–119, May 2002.
[31] L. Du, Y. Liu, Y. Li, and C. Li, "Effect of ultrasonic treatment on SU-8 swelling in UV-LIGA technology," *Opt. Precis. Eng.*, vol. 20, no. 9, pp. 2006–2013, Sep. 2012.
[32] S. K. Griffiths, J. Crowell, B. L. Kistler, and A. S. Dryden, "Dimensional errors in LIGA-produced metal structures due to thermal expansion and swelling of PMMA," *J. Micromech. Microeng.*, vol. 14, no. 11, pp. 1548–1557, Aug. 2004.
[33] H.-K. Chang and Y.-K. Kim, "UV-LIGA process for high aspect ratio structure using stress barrier and C-shaped etch hole," *Sens. Actuators A, Phys.*, vol. 84, no. 3, pp. 342–350, May 2017.
[34] H. Cao, K. Zhou, X. Chen, and X. Zhang, "Early chatter detection in end milling based on multi-feature fusion and 3σ criterion," *Int. J. Adv. Manuf. Technol.*, vol. 92, nos. 9–12, pp. 4387–4397, Oct. 2017.
[35] Y. Qin, L. Chen, Y. Hao, S. Liu, and Z. Xian, "A study on the elastic coefficients of setback micro-springs for a MEMS safety and arming device," *Microsyst. Technol.*, to be published. [Online]. Available: https://link.springer.com/article/10.1007/s00542-019-04558-1#aboutcontent

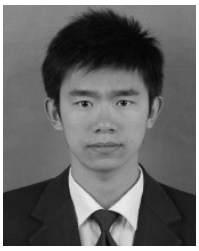

YU QIN was born in Dandong, Liaoning, China, in 1990. He received the M.E. degree in mechanical engineering from the Dalian Jiaotong University, Dalian, China, in 2015. He is currently pursuing the Ph.D. degree in mechanical engineering with Northeastern University, Shenyang, China.

His research interests include the application of micro-springs, and the design of MEMS safety and arming device.

LIANGYU CHEN was born in Weifang, Shandong, China, in 1959. He received the B.E. degree in mechanical engineering from the China University of Petroleum, Dongying, China, in 1982, and the M.E. and Ph.D. degrees in mechanical engineering from Northeastern University, Shenyang, China, in 1986 and 1994, respectively.

Since 1997, he has been a Professor with the School of Mechanical Engineering and Automation, Northeastern University. He is the author of 12 books and more than 80 articles. His research interests include structural integrity of metallurgical equipment, mechanical power transmission and transmission technology, and engineering equipment modeling and digital technology.

YONGPING HAO was born in Shenyang, Liaoning, China, in 1960. He received the Ph.D. degree in mechanical engineering from the Beijing Institute of Technology, Beijing, China, in 2004.

He is currently a Professor with Shenyang Ligong University. His research interests include applied information technology, and microsystems application technology.

SHUANGJIE LIU was born in Zhoukou, Henan, China, in 1980. She received the Ph.D. degree in mechanical engineering from the Changchun University of Science and Technology, Changchun, China, in 2013.

She is currently an Associate Professor with Shenyang Ligong University. Her research interests include the design of MEMS inertial devices, and simulation and machining techniques.

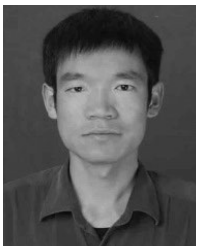

XIANLONG HU was born in Fuping, Shaanxi, China, in 1980. He received the B.E. degree in automation from the Northwestern Polytechnical University, Xi'an, China, in 2004.

Since 2004, he has been with Huaihai Industries Group Company Ltd. His research interests include micro-miniature explosive train, and the manufacture of MEMS safety and arming device.